MAP2c, but Not Tau, Binds and Bundles F-Actin via Its Microtubule Binding Domain

Benoit Roger,[1,3] Jawdat Al-Bassam,[2,3]
Leif Dehmelt,[1] Ronald A. Milligan,[2]
and Shelley Halpain[1,*]
[1]Department of Cell Biology and
Institute for Childhood and Neglected Diseases
[2]Center for Integrative Molecular Biosciences
The Scripps Research Institute
10550 North Torrey Pines Road
La Jolla, California 92037

Summary

Background: MAP2 and tau are abundant microtubule-associated proteins (MAPs) in neurons. The development of neuronal dendrites and axons requires a dynamic interaction between microtubules and actin filaments. MAPs represent good candidates to mediate such interactions. Although MAP2c and tau have similar, well-characterized microtubule binding activities, their actin interaction is poorly understood.
Results: Here, we show by using a cosedimentation assay that MAP2c binds F-actin. Upon actin binding, MAP2c organizes F-actin into closely packed actin bundles. Moreover, we show by using a deletion approach that MAP2c's microtubule binding domain (MTBD) is both necessary and sufficient for both F-actin binding and bundling activities. Surprisingly, even though the MAP2 and tau MTBDs share high sequence homology and possess similar microtubule binding activities, tau is unable to bind or bundle F-actin. Furthermore, experiments with chimeric proteins demonstrate that the actin binding activity fully correlates with the ability to promote neurite initiation in neuroblastoma cells.
Conclusions: These results provide the first demonstration that the MAP2c and tau MTBD domains exhibit distinct properties, diverging in actin binding and neurite initiation activities. These results implicate a novel actin function for MAP2c in neuronal morphogenesis and furthermore suggest that actin interactions could contribute to functional differences between MAP2 and tau in neurons.

Introduction

Coordination between microtubules and actin filaments is an essential component of cell morphogenesis [1]. Such coordination is particularly important in neuronal development, where growth cone-tipped axons and dendrites form and elongate from the cell body in response to extracellular signals [2–4]. Several candidate proteins that might physically and functionally link these polymer systems have been identified, including the "classical" microtubule-associated proteins (MAPs).

MAP2 and tau are among the most abundant neuronal MAPs. In mammals several splice variants of MAP2 and

*Correspondence: shelley@scripps.edu
[3]These authors contributed equally to this work.

tau derive from two distinct genes that are highly conserved across species. They contain homologous C-terminal domains and divergent N termini [5]. MAP2 and tau have well-characterized microtubule binding activities, conferred by their highly conserved C-terminal microtubule binding domain (MTBD), which consists of three or four 31-residue repeats. Their binding increases microtubule stability by reducing the frequency of catastrophe and increasing the frequency of rescues [6–8].

Multiple studies have suggested that MAP2 and tau interact with actin filaments in vitro [9–15]. However, the nature of this interaction and its physiological relevance is poorly understood. In the series of studies described below we provide the first extensive characterization of F-actin binding for MAP2c and tau. Contrary to earlier suggestions, our results indicate that only MAP2c exhibits direct binding to F-actin. Deletion analysis was used to map the domain responsible for F-actin binding, and a cellular model of neurite initiation was used to investigate its functional relevance.

Results

We used bacterially expressed MAPs to obtain homogenous material for study. Previous studies used material purified from brain or from eukaryotic expression systems and may have been a mixture of different isoforms and/or proteins with posttranslational modifications. The sequences of MAP2 and tau contain numerous serines and threonines that are potential targets for several kinases [5], so native protein or protein from eukaryotic expression systems may be heterogeneously phosphorylated. Binding assays were conducted by using physiological ionic strength buffer, because ionic strength significantly influences MAP-polymer interactions (B.R., J.A.-B., R.A.M., and S.H., unpublished data; see also [16]). Although previous studies used skeletal muscle α-actin, here we used platelet actin, which is a mixture of β and γ isoforms. These are the only isoforms expressed in neurons [17] and, therefore, the isoforms that the MAPs will encounter in vivo. We felt this was important because actin properties exhibit isoform specificity [18]. The above factors may explain differences between our observations and earlier studies.

MAP2c Binds Both F-Actin and Microtubules
Cosedimentation assays were used to compare binding of MAP2c to microtubules versus F-actin. Binding curves were generated by incubating increasing amounts of MAP2c with a fixed amount of microtubules or F-actin. Recombinant MAP2c bound both F-actin and microtubules directly (Figure 1A). Microtubule binding data fit best to a single-site binding model, whereas actin binding curves were biphasic, with an initial phase of high-affinity, saturable binding and a second phase that was linear and nonsaturable (Figure 1B). Curve fitting and statistical analysis yielded an apparent K_D for the high-affinity phase of MAP2c F-actin binding of 0.4 ± 0.05

A

B
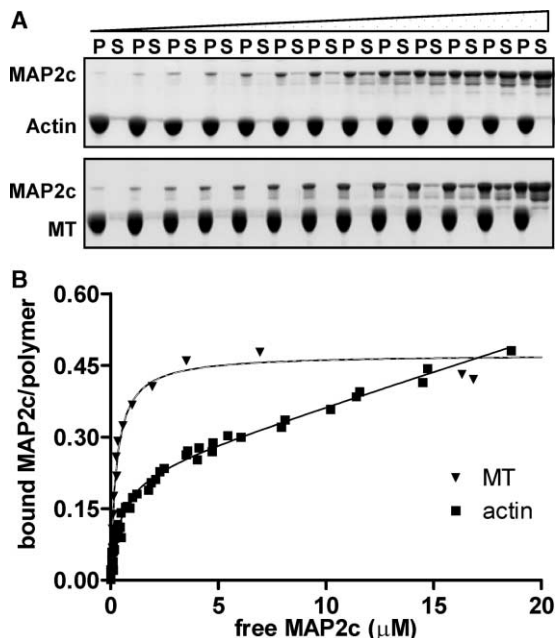
Figure 1. MAP2c Binds to Microtubules and Actin with Different Characteristics

(A) Cosedimentation assay of MAP2c with F-actin and microtubules. Increasing amounts of MAP2c were mixed with a fixed amount of actin (top) or microtubules (bottom), incubated for 1 hr, and then centrifuged at high speed to pellet the cytoskeletal polymer and associated protein. A sample of the pellets (P) and supernatant (S) were separated on a 10% poly-acrylamide gel and stained with BioSafe Coomassie. Some degradation products are visible at high concentrations. The gels were then dried and scanned using a densitometer to generate the binding curves shown in (B). The results of independent experiments were plotted on a graph and fitted to a one-site binding model (microtubule) or a one-site model followed by a linear, nonsaturable trend model (actin) with Prism software.

μM, a value close to the K_D value of 0.3 ± 0.03 μM we calculated for MAP2c microtubule binding (Table 1).

Next, we used deletion mutants (see Figure 2A) to determine which MAP2c domains were critical for F-actin binding. Protein lacking the MAP2c N terminus (ΔN), C terminus (ΔC), and MTBD (ΔMTBD) or protein containing the MTBD alone (ΔN + C) were generated and used in cosedimentation assays with F-actin. Previous work established that the MTBD contains the high-affinity microtubule binding activity of MAP2 [19], a result

we confirmed here (data not shown). This region of MAP2c also proved to contain the F-actin binding activity, since the MTBD alone (ΔN + C) as well as both the ΔN and ΔC mutants bound F-actin with similar affinity and biphasic binding behavior as was observed by using the full-length protein (Figure 2B). In contrast, the ΔMTBD protein showed only nonsaturable binding to F-actin (Figure 2B). These results demonstrate that the MAP2c MTBD is both necessary and sufficient for F-actin binding.

MAP2c MTBD Bundles Actin Filaments

Data from viscometry and rheometry assays previously suggested that MAP2c induces F-actin crosslinking [9, 11, 15]. We used cryo-electron microscopy (cryo-EM) to investigate the nature of the MAP2c-actin interaction. In the absence of MAP2c, actin filaments were randomly distributed over the grid (Figure 3A, panel I). In contrast, F-actin bound with full-length MAP2c was observed in closely packed bundles (Figure 3A, panels II and IV). Analysis of diffraction patterns of selected cryo-EM images indicated that actin filaments were spaced regularly, 86Å apart (Figure 3A, panel V). At this spacing, the ridges of each actin filament touch those of neighboring filaments. Similar bundling of filaments was observed with the MTBD alone (ΔN + C) and with the ΔN and ΔC deletion mutants (data not shown). However, the construct lacking the MTBD (ΔMTBD) had no bundling ability, and in its presence actin filaments were randomly distributed over the grid (Figure 3A, panel III).

To determine the stochiometry required for bundling, we used a differential-speed sedimentation assay [20]. Increasing amounts of MAP2c were incubated with F-actin, then sedimented at low speed (5000 × g) to sediment actin bundles (Pellet of bundles, P_B). Filaments remaining in the supernatant were then sedimented (Pellet of filaments, P_F) by centrifugation at high speed (190,000 × g). Unbound MAP2c remained in the supernatant (S). In this assay F-actin alone was not found in P_B and was entirely present in P_F. However, in the presence of increasing amounts of full-length MAP2c, the proportion of actin in bundles (P_B) increased progressively, with a concomitant decrease in actin remaining as individual filaments (P_F; Figure 3B). MAP2c bundling activity was calculated as the fraction of actin in P_B measured for a range of MAP2c:actin molar ratios [20]. One MAP2c per 20 actin subunits was sufficient to in-

Table 1. Biochemical Binding Parameters of Wild-Type and Chimeras

	Microtubule		F-Actin		
	Max Bound/Tubulin	K_D (μM)	Max Bound/Actin	K_D (μM)	P Value
Wt MAP2c	0.48 ± 0.01	0.3 ± 0.03	0.23 ± 0.01	0.4 ± 0.05	15.9 ± 1.5
4r-tau	0.29 ± 0.02	0.1 ± 0.05	NA	NA	NA
3r-tau	0.25 ± 0.01	0.5 ± 0.06	NA	NA	NA
MAP2 chimera	0.40 ± 0.02	0.5 ± 0.12	0.47 ± 0.05	9.9 ± 2.01	249051
Tau chimera	0.49 ± 0.03	0.6 ± 0.14	0.13 ± 0.03	0.3 ± 0.22	9.7 ± 4.6

MAP2c chimera refers to a MAP2c construct having tau's MTBD. Tau chimera corresponds to a tau construct having MAP2c's MTBD (see Experimental Procedures). P describes the linear second phase of the curve that presumably reflects self-association of MAP2c. It is similar to a K_D but no saturation is observed [16]. NA indicates that binding parameters could not be determined due to lack of saturable binding.
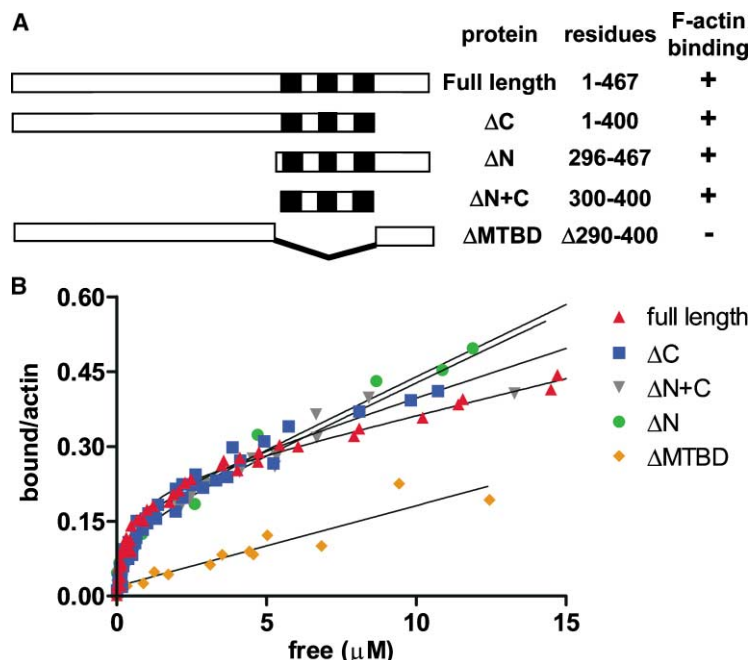
Figure 2. Mapping of MAP2c's Actin Binding Domain

(A) Representation of the different deletion mutants used to map the actin binding activity of MAP2c. The microtubule binding repeats are shown as black boxes. Residue numbers and actin binding are also indicated for each construct.

(B) Actin binding curves were generated from cosedimentation assays for each construct. All the deletion mutants containing the MTBD bound to actin in a similar way as the full-length protein.

duce complete bundling (Figure 3C). This ratio is 5-fold lower than the maximum MAP2c-actin binding stoichiometry in the initial phase of MAP2c binding, suggesting that a small number of MAP2c molecules is sufficient to induce the bundling of essentially all actin filaments present in the reaction. The bundling behavior of the ΔN, ΔC, and ΔN + C mutants was indistinguishable from that of the full-length protein, and no bundling was observed with the ΔMTBD mutant (Figure 3C). Together, these data show that both actin binding and bundling activities are properties of the MAP2c MTBD.

Tau Isoforms Do Not Bind F-Actin
The amino acid sequences within the MTBD of MAP2c and tau are 80% homologous (67% identical; see sequence alignment in Figure S1). We therefore expected tau to exhibit actin binding properties similar to those of MAP2c. Surprisingly, this was not the case. Cosedimentation of microtubules with increasing concentrations of a tau isoform containing three repeats in its MTBD (3r-tau) showed that the binding is specific and saturable, similar to that of MAP2c (compare Figure 4A with Figure 1A). However, 3r-tau did not bind F-actin with high affinity and remained largely in solution (Figure 4B). We also assayed the actin binding activity of four-repeat tau (4r-tau), as well as that of native bovine brain tau. As expected, like MAP2c and 3r-tau, 4r-tau bound microtubules with high affinity (Table 1); however, neither native tau, 3r-tau, nor 4r-tau bound saturably to F-actin (Figure 4C). These data demonstrate that even though the tau and MAP2c MTBDs are highly homologous and have similar microtubule binding affinities, their actin binding affinities are extremely different.

The MAP2c MTBD Confers F-Actin Binding and Bundling Activities to Tau
The lack of F-actin binding activity in tau compared to MAP2c could be due either to intrinsic sequence

differences in their MTBDs, or to other domains in tau that interfere with its actin interaction. To distinguish these possibilities we generated chimeric proteins in which the MTBD sequences of MAP2c and 3r-tau were swapped. A chimera containing the MAP2c N- and C-terminal domains fused on either side of the tau MTBD bound very poorly to F-actin (20-fold less than full-length MAP2c) and did not bundle the filaments (Figures 5A and 5C, Table 1). In contrast, a protein containing the N- and C-terminal domains of tau plus the MAP2c MTBD was very similar to full-length MAP2c in its actin binding and bundling properties (Figures 5B and 5C, Table 1). These data demonstrate that the difference in binding (and bundling) activities between MAP2c and tau must be entirely due to sequence differences within the MTBD.

Actin Binding Activity Is Necessary for Neurite Initiation in Neuro-2a Cells
To address the functional relevance of the MAP2's actin interaction, we tested various constructs in a neurite initiation assay in the neuroblastoma cell line Neuro-2a. Previously, we demonstrated that neurites in these cells share key features with primary neurons, and thus represent an appropriate yet accessible model system for studies of neurite initiation [4, 21]. Neuro-2a cells form neurites upon differentiation induced by retinoic acid [22]. However, MAP2c by itself is sufficient to promote neurite formation when transfected into these cells, even without retinoic acid induction [21]. The effects of retinoic acid and MAP2c are not additive, suggesting that they share the same biochemical mechanism (Figure 6B).

Neuro-2a cells were transfected with GFP alone or GFP-tagged MAP2c, 3r-tau, or chimeric proteins and analyzed 24 to 48 hr later for the presence of neurites (Figure 6). Transfection of the cells with each of the MAP-containing constructs resulted in a prominent stabilization of interphase microtubules, leading to their
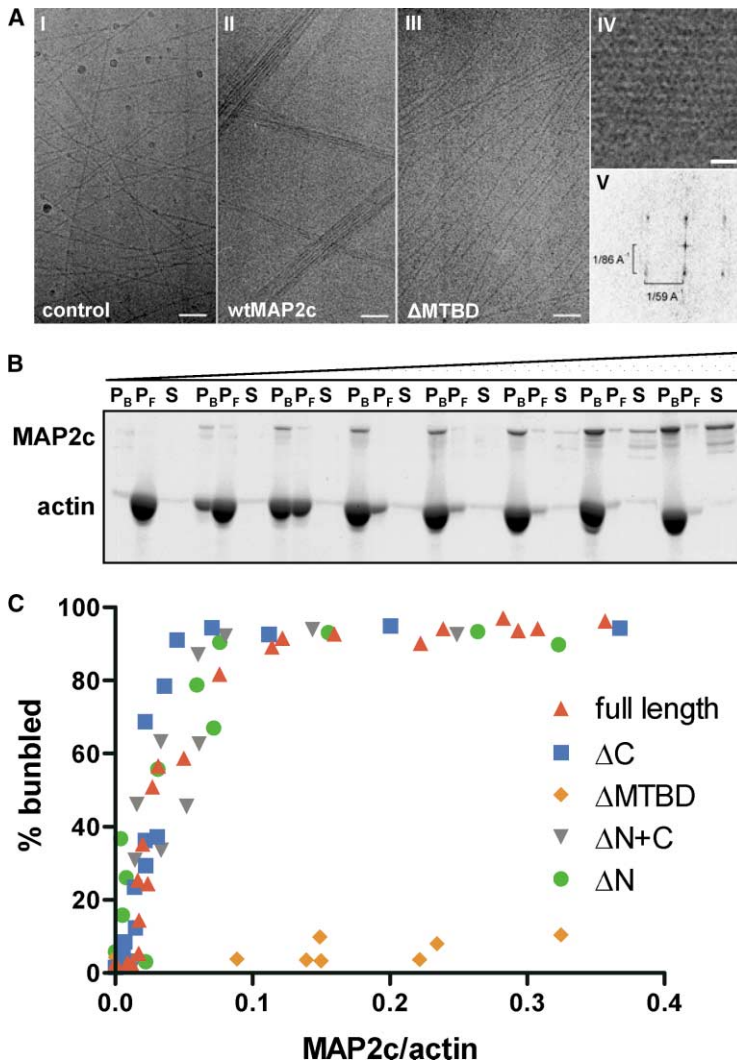
Figure 3. MAP2c Organizes F-Actin into Closely Packed Bundles via Its MTBD

(A) Cryo-EM micrographs showing MAP2c-induced bundling of F-actin. Panel I, F-actin only; panel II, bundles induced by full-length MAP2c; panel III, random distribution similar to panel I found with ΔMTBD protein; panel IV, enlarged view of actin bundle; panel V, diffraction pattern from the bundle shown in Panel IV; the spacing between filaments is 1/86 Å^{-1} and the pitch of the actin helix is 1/59 Å^{-1}. Scale Bar is 100 nm in panels I–III, 20 nm in panel IV.

(B) Differential sedimentation assay of actin bundling induced by MAP2c. Increasing amounts of MAP2c were added to F-actin. After incubation, mixtures were first centrifuged at low speed to pellet actin bundles (P_B). The supernatants were then centrifuged at high speed to pellet remaining actin filaments (P_F). An aliquot of each fraction (P_B, P_F, and S, remaining supernatant) was then separated on a gel and stained. Note that 100% bundling is obtained before MAP2c saturates F-actin and appears in the supernatant.

(C) Gels were scanned with a densitometer and results were plotted as the percentage of bundling versus MAP2c/actin molar ratio for each construct. All deletion mutants that bound to F-actin also carried the bundling activity.

accumulation into large bundles (Figure 6A, bottom row). In contrast, untransfected cells and GFP-transfected cells contained a normal array of nonbundled microtubules. Furthermore, only 5%–10% of the control GFP transfected cells exhibited neurite-like processes, similar to nontransfected cells. This percentage increased to 30%–40% in cells transfected with GFP-MAP2c, a level comparable to that of neurite induction by retinoic acid (Figure 6B). In contrast, 3r-tau completely lacked this neurite induction activity. In addition, the MAP2c chimera, which contains tau's MTBD, was inactive in neurite initiation, although it was clearly able to stabilize microtubules into bundles (Figures 6A and 6B). On the other hand, the tau chimera bearing the MAP2c MTBD, which is capable of binding F-actin, induced neurites to a similar extent as MAP2c. Since neurite initiation completely correlated with the actin binding activity of the different constructs in vitro, yet all MAPs stabilized microtubules to the same extent, we conclude that neurite initiation by MAP2c requires its interaction with F-actin.

Discussion

Actin Binding and Microtubule Binding Are Mediated by a Single Domain in MAP2c

MAP2c exhibits monophasic binding to microtubules, with the data fitting well to a single-site binding model. Conversely, MAP2c binds F-actin with biphasic behavior, consistent with initial single-site binding followed by a weaker, nonsaturable binding phase. Similar biphasic binding was previously described for tau interaction with microtubules. In this instance, the model proposed was initial specific binding followed by aggregation of tau on the microtubule surface [16, 23]. This seems a plausible explanation also for MAP2c-actin interactions.

By using deletion mutants, we found that the MTBD of MAP2c is both necessary and sufficient for its actin binding activity. MAP2c is largely disordered in solution [24] but adopts an ordered conformation when it binds microtubule protofilaments [25]. Actin filaments are quite different from microtubules in terms of overall geometry, monomer spacing, and surface characteristics.
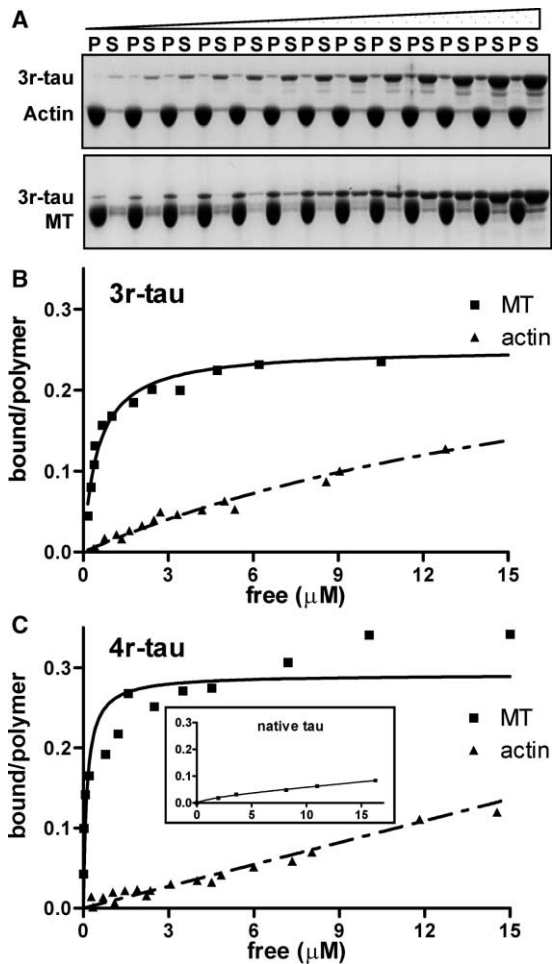
Figure 4. Tau Does Not Bind Saturably to F-Actin

(A) Cosedimentation assay of 3r-tau with F-actin (top) and microtubules (bottom).

(B) Binding curves for 3r-tau to actin (triangles) versus microtubules (squares).

(C) Binding curves for 4r-tau to actin (triangles) versus microtubules (squares). Inset, actin binding curve for native tau. Note that all three tau preparations exhibited only nonsaturable binding to F-actin.

Since the same domain of MAP2c is involved in binding to both polymers, it implies that this region can assume different specific conformations, depending on the binding partner. Presumably, the natively unfolded structure of MAP2c permits adoption of different folds, leading to unique, stable conformations determined by the initial collision complex with the substrate. It seems likely that distinct residues within the MTBD of MAP2c mediate microtubule binding versus actin binding.

The direct overlap of the microtubule and F-actin binding activities in the MTBD suggests that each MAP2c molecule can bind either a microtubule or an actin filament. However, the MTBD is not likely to bind both microtubules and F-actin at the same time, since we observe that microtubules compete for MAP2c in F-actin bundling assays (B.R., J.A.-B., R.A.M., and S.H., unpublished data). However, we cannot rule out the possibility that a MAP2c molecule bound to a microtubule could dimerize with a MAP2c molecule bound to an actin filament to crosslink the two polymers. The overlap in microtubule and actin binding domains is unique so far among cytoskeletal crosslinkers. For example, MAP1B and plectin utilize entirely distinct binding domains for binding different polymers [26, 27], and although BPAG1 utilizes overlapping regions of the molecule for binding actin and microtubules, conversion of the microtubule binding domain to an actin binding domain requires alternative RNA splicing [28].

The MAP2 MTBD Both Binds and Bundles F-Actin

F-actin crosslinking by MAP2 was previously reported [9, 12, 15]; however, a surprising finding from our study is that the F-actin bundling activity is fully contained within the MAP2 MTBD. Differential speed sedimentation analysis establishes that actin bundling activity in MAP2c is robust and that one MAP2c per 20 actin monomers is sufficient to induce complete actin bundling. This ratio is similar to that for other well-characterized actin filament crosslinkers, such as α-actinin [20].

The MAP2c actin bundling activity may result either from the presence of multiple actin binding sites within the MAP2c MTBD or a single actin binding site coupled with the ability of the MAP2c MTBD to dimerize. Our data favor the second model. First, the initial binding curve fits a single-site binding model, so two actin binding sites per MAP2c seems unlikely. In addition, there is evidence that full-length MAP2c [29] and its MTBD [30] can self-associate in solution. Self-association of MAP2c bound to F-actin could explain the second, nonsaturable phase of actin binding. Finally, if we force our data to a two-site binding model, the K_D for the second binding site appears to be too low ($\sim$40 μM) to account for the high bundling efficiency we observe. Together these observations are consistent with specific binding followed by weak self-association activity. In this model, the MTBD would first bind to individual actin filaments, taking up its actin-specific conformation. A weak affinity between exposed surfaces of this actin-specific MTBD conformation would result in interactions between adjacent actin filaments, effectively zipping them together into bundles.

Tau MTBD Lacks Actin Binding, Correlated with Its Inability to Initiate Neurites

Because the MAP2c and tau MTBDs are highly homologous, it was surprising to find that this homology did not translate into a matching ability to bind F-actin. Since previous studies suggested that tau could interact directly with F-actin [9, 13, 14], we additionally tested tau's ability to bind to F-actin polymerized from skeletal muscle α-actin in our cosedimentation assays. In contrast to MAP2c, which saturably bound filaments prepared from either α-actin or β/γ-actin, tau did not bind saturably to F-actin from either source (see Figure S2).

By using a domain swapping strategy, we found that the MAP2c MTBD confers actin binding and bundling activities on tau, whereas the tau-MTBD dramatically abolishes these activities in MAP2c. This suggests that lack of actin binding activity in tau is not due to inhibitory

A

Protein	F-actin binding (µM)
MAP2c	0.4±0.05
tau	NA
MAP2c Chimer	9.9±2.01
tau Chimer	0.3±0.22

B

C
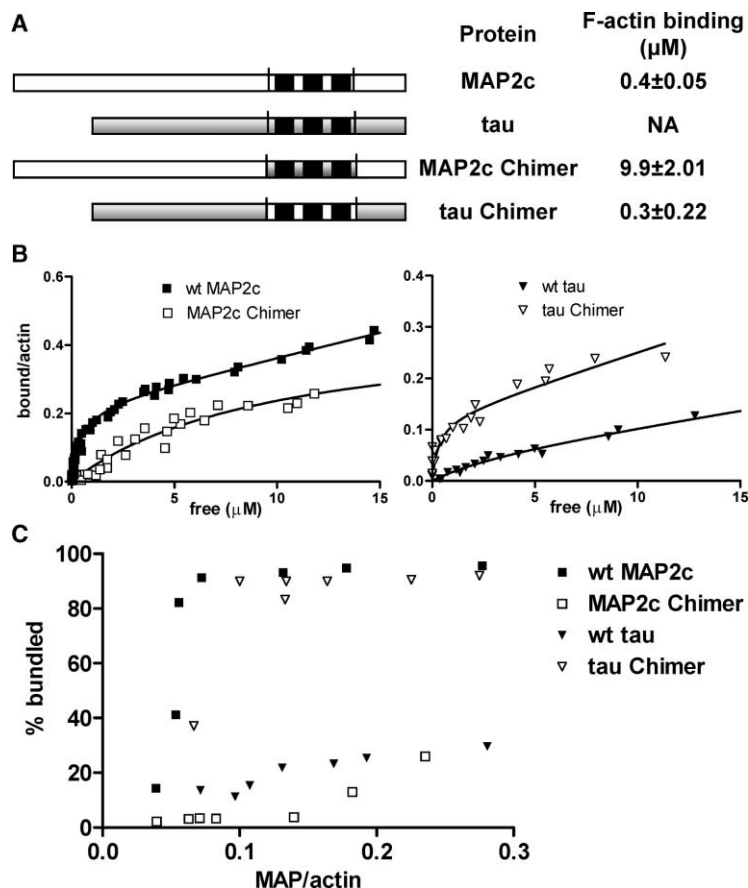
Figure 5. The MTBD of MAP2c Confers Actin Binding Activity to Tau

(A) Representation of the wt and chimeric proteins used. Mutations were introduced outside the microtubule binding domain of MAP2c and 3r-tau to generate the chimeras. These point mutations did not affect binding behavior of the proteins (not shown).

(B) Actin binding curves for the different chimeras compared to the corresponding wt proteins. The MAP2c-MTBD confers actin binding to tau, whereas tau-MTBD inhibits actin binding of MAP2c. Microtubule binding of both chimeras where unchanged (not shown).

(C) Bundling curve (as in Figure 3C) for these chimeras. The MAP2c-MTBD not only conferred actin binding to tau chimer, but it also conferred bundling activity. On the other hand, MAP2c chimer lost its ability to bundle F-actin efficiently.

effects mediated by other parts of the tau molecule but, rather, is due to an intrinsic lack of binding activity in its MTBD. The nonidentical residues within the MTBD of tau versus MAP2c must play critical roles in their divergent F-actin affinities.

Even though MAP2 and tau share similar microtubule-stabilizing activities, their cellular functions are presumably not redundant. In mature neurons, MAP2 is restricted to the cell body and dendrites, while tau is mainly in the axon. Experiments that use antisense RNA inhibition implicate MAP2, but not tau, in neurite initiation but suggest that tau has a role in the development of neuronal polarity by influencing specification of the axon [31–33]. Such differences in the targeting and function of MAP2 versus tau were presumed to be mediated by their widely divergent N termini. Our results suggest, however, that even the MTBD might mediate functional differences in MAP2 versus tau.

Indeed, the lack of actin binding activity in tau correlates with the absence of activity in our neurite initiation assay. Biernat et al. reported that tau stimulates neurite outgrowth in the same Neuro-2a cell system we used here [34]. However, in their assay, cells were induced to differentiate using retinoic acid before being transfected with recombinant tau. Thus, it seems likely that tau stabilizes microtubules to promote neurite elongation once neurites have been initiated but lacks an essential activity to kick-start the process.

Another interesting difference between tau and MAP2

is evident in human pathology. Tau's aggregation into paired helical filaments is a hallmark of neurodegenerative tauopathies and Alzheimer's disease [35]. Tau aggregates into similar paired helical filaments in vitro under specific conditions, and the MTBD region of tau clearly mediates this effect [36]. However, even though MAP2 can aggregate into filaments under similar in vitro conditions [30], there has been little evidence to date that MAP2 is present in pathological aggregates in vivo. Given the divergence in actin binding activity within the tau and MAP2 MTBDs, it is tempting to speculate that MAP2 may be somehow protected from aggregation in vivo due, for example, to its ability to interact with F-actin or to adopt alternative folding pathways not available to tau.

Functional Implications for MAP2c-Actin Interaction

Neurite initiation involves a rearrangement in the cortical actin network accompanied by microtubule accumulation and bundling at the site of the rearrangement [4]. MAPs that interact with both polymers are among the many proteins that may act to coordinate these cytoskeletal changes. Expression of MAP2c in Neuro-2a cells is sufficient to promote neurite initiation [21]. However, the use of taxol to mimic the MAP2c-induced stabilization of microtubules, by itself, is not. Stabilization of microtubules by taxol must also be accompanied by a treatment interfering with actin dynamics for neurite-like

A

B
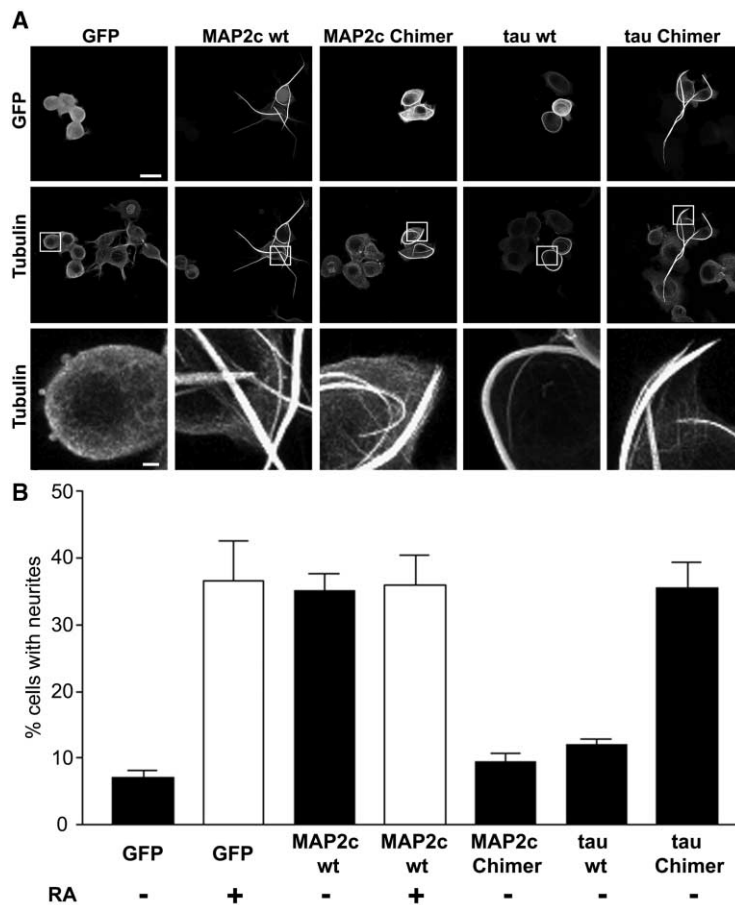
Figure 6. Actin Binding Activity Is Necessary to Induce Neurite Formation in Neuro-2a Cells

(A) Neuro-2a cells were transfected with the indicated GFP-tagged constructs, fixed after 2 days, and stained for tubulin. The bottom row shows an enlarged view of the region boxed in the center row, illustrating that all constructs except GFP alone induced a reorganization of the microtubule network. Only the constructs able to bind F-actin induced neurite formation. Top and middle rows, scale bar is 10 μm. Bottom row, scale bar is 1 μm. (B) Quantification of the neurite initiation activity for the different constructs and treatments. Pluses and minuses indicate whether the culture was incubated with retinoic acid (RA). At least 500 cells from three independent experiments were counted for each construct and scored for having neurite-like processes. A process was defined as a thin extension the length of at least one cell body diameter. Data represent mean ±SEM.

process formation to take place [21]. These observations strongly suggest that MAP2c utilizes actin binding activity either directly or indirectly in mediating neurite initiation. The present results demonstrating high-affinity binding between MAP2c and F-actin unequivocally demonstrate the potential for MAP2c to interact directly with actin filaments. In contrast to MAP2c, tau appears to lack the ability to stimulate neurite initiation. Our data suggest that the difference in neurite initiation activities between MAP2 and tau is not due to any difference in their microtubule stabilizing activities but, rather, involves the dramatic disparity in their ability to bind actin filaments.

The comparable affinity of MAP2c for actin and microtubules is puzzling, since MAP2c colocalizes predominantly with microtubules in neurons [37] even though it can also be found in association with actin filaments [38]. There are several possible explanations for the apparent preferential location on microtubules. First, MAP2c's actin and microtubule binding activities are probably regulated in vivo by posttranslational events like phosphorylation [5, 39]. The interaction of MAP2c with actin might therefore be transient, and only a small fraction of MAP2c might exist in association with F-actin at any given time. Second, MAP2c localization on actin could be restricted to regions within the neuron where the distribution of microtubules and F-actin substantially overlap, such as the neuronal growth cone, where F-actin

and microtubules modulate each other's behavior [3, 4, 40]. MAP2c, via its dual binding activities, could play a role in the coupling of microtubule and actin filament dynamics.

Conclusion
Our results suggest that the actin binding activity contained within the MTBD of MAP2 is functionally relevant in neuronal morphogenesis. Furthermore, the lack of this activity in tau contributes to important functional distinctions between these closely related microtubule-associated proteins.

Experimental Procedures

Constructs
Chimeras were produced by PCR amplification of N terminus, MTBD, and C terminus fragments of MAP2c and 3r-tau by using the following primers:

MAP2c N terminus, 5′-GGAATTCCATATGGCTGACGAGAGG-3′ and 5′-GGAATTCGCTTGGGAGTAGCTGGGGAC-3′; MAP2c MTBD, 5′-GGAATTCGGCTCATTAACCAACC-3′ and 5′-GGGGTACCACCTC CAGGTACATG-3′; MAP2c C terminus, 5′-GGGGTACCGTGAAG ATTGACAGCCAAAAG-3′ and 5′-CGGGATCCTCACAAGCCCTGCT TAG-3′; Tau N terminus, 5′-GGAATTCCATATGGCTGAGCCCCG-3′ and 5′-GGAATTCGGCTCTTGGCGGAAGACGG-3′; Tau MTBD, 5′-GGAATTCAGACAGCCCCCGTGCCCATG-3′ and 5′-GGGGTACCT CCGCCAGGGACGTG-3′; Tau C terminus, 5′-GGGGTACCAAAAA GATTGAAACCCAC-3′ and 5′-CGGGATCCTCACAAACCCTGCTT GGC-3′.

All fragments were subcloned into a pUC19 plasmid by using NdeI and EcoRI for N terminus constructs, EcoRI and KpnI for MTBD constructs, and KpnI and BamHI for C terminus constructs. These pUC19 subclones were then used to generate the corresponding fragments to reconstitute full-length protein or to produce chimeras in the pET15b vector for bacterial expression and into the peGFP-C3 vector for transfection into Neuro-2a cells. To correctly position the MTBDs in these proteins, mutations in two residues were introduced outside the MTBD of MAP2c and tau. Protein containing these two residue changes served as controls and behaved similarly to wild-type protein (data not shown). All constructs were sequenced before use.

Expression and Purification of MAP2 Proteins

Native tau (bovine brain) was purchase from Cytoskeleton Inc., Denver, CO. Recombinant MAPs were expressed and purified from cDNA constructs in pET3a, pET30a, and pET15b plasmids (this work; [39, 41]). Proteins were produced and prepared as described in [25]. Purified MAPs were dialyzed against PEMD buffer (100 mM PIPES [pH 6.8], 1 mM EGTA, 1 mM MgCl$_2$, 1 mM DTT) prior to experiments. Protein concentration was measured using BCA protein assay (Pierce Biotechnology, Inc., Rockford, IL) and/or by quantitative densitometry of Coomassie-stained SDS-PAGE gels and comparison to known standards.

Microtubule and Actin Cosedimentation Assays

Microtubules were prepared from tubulin (Cytoskeleton, Inc., Denver, CO) by the addition of GTP and taxol and incubation for 20 min at 34°C. Platelet actin was purchased from Cytoskeleton, Inc. and polymerized by addition of KCl and ATP. Binding reactions were mixed in 50 μl PEMD buffer at either 8.2 μM tubulin or 15 μM actin with varying concentrations of MAP protein. Reactions were incubated 1 hr at ambient temperature and then centrifuged at 190,000 × g for 15 min. Supernatants and pellets were separated and brought to equal volumes in SDS sample buffer. Equal volumes of supernatants and pellets were analyzed by SDS-PAGE. Coomassie-stained gels were dried and analyzed by quantitative densitometry on a personal densitometer (Molecular Dynamics, Amersham Biosciences Corp., Piscataway, NJ). The ratio of the MAP intensity to actin or tubulin intensity was corrected for their respective molecular weights. The MAP to actin ratio was plotted versus the free MAP concentration and curves fitted to the experimental data with Prism software (GraphPad Software, Inc., San Diego, CA) by using a biphasic binding model [16]. This biphasic binding model consists of an initial single-site binding phase followed by a linear nonspecific binding phase. Student's t tests to evaluate the differences between binding parameters were performed in Prism by using standard error values associated with the nonlinear regression. Identical conclusions were derived from experiments in which microtubule or F-actin concentrations were held constant and MAP concentration was varied (data not shown).

Sample Preparation and Cryo-Electron Microscopy

The MAP/F-actin mixtures at either saturating or nonsaturating concentrations were prepared for electron microscopy as previously described [25] and examined on a Philips CM200T FEG electron microscope. Electron micrographs were recorded under low-dose conditions (<10 e/Å^2 total dose) at an operating voltage of 120 kV at a nominal magnification of 38,000.

Differential Speed Sedimentation Analysis of Actin-Bundling Activity

F-actin was incubated in the presence and absence of various concentrations of MAP protein for 1–2 hr at ambient temperature. The MAP/F-actin mixtures were then centrifuged at low speed at 5000 × g for 10 min to separate actin bundles that pellet (P$_B$) from actin filaments [20]. The supernatant was removed and spun at high speed (190,000 × g, 15 min) to sediment unbundled actin filaments (P$_F$). The P$_B$, P$_F$, and the final supernatant (S) were all brought to equal volumes with SDS sample buffer and analyzed as described above. The percentage of bundled actin was determined as a ratio of P$_B$ to the total actin (P$_B$ + P$_F$).

Cell Culture, Neurite Initiation Assay, and Immunocytochemistry

Neuro-2a cells were cultured by using standard conditions [22]. Transfection and neurite detection and quantification was performed as described [21]. For imaging, cells were plated on poly-L-lysine-coated coverslips. After the experiment, cells were fixed with 0.3% glutaraldehyde in Phosphate Buffer Saline (PBS) for 10 min, permeabilized with 0.5% Triton X-100 in PBS for 10 min, treated with 0.1% NaBH$_4$ for 10 min, then with 0.1 M glycine in PBS for 20 min, and incubated 30 min at 37°C with 10% bovine serum albumin (BSA) in PBS. Cells were stained with a rabbit polyclonal anti-tubulin antibody (βIII-tub at 1:2000 dilution [a gift from A. Frankfurter]) in 2% BSA/PBS for 2 hr at room temperature. Anti-rabbit IgG antibody conjugated to Alexa 568 (1:1000 Molecular Probes) was used as secondary in 2% BSA/PBS for 1 hr at room temperature. Image acquisition was performed by using an Olympus Fluoview 500 laser scanning confocal microscope. Images were processed for display with Adobe Photoshop and correspond to maximum projection images from stacks of z series collected throughout the cell (35–45 sections; 0.25 μm steps). All images were acquired by using the same collection parameters for quantitative comparisons.

Supplemental Data

Supplemental Data including sequence alignment of MAP2c and tau's MTBD as well as binding curves generated from muscle α-actin are available at http://www.current-biology.com/cgi/content/full/14/5/363/DC1/.

References

1. Goode, B.L., Drubin, D.G., and Barnes, G. (2000). Functional cooperation between the microtubule and actin cytoskeletons. Curr. Opin. Cell Biol. *12*, 63–71.

2. Fuchs, E., and Karakesisoglou, I. (2001). Bridging cytoskeletal intersections. Genes Dev. *15*, 1–14.

3. Schaefer, A.W., Kabir, N., and Forscher, P. (2002). Filopodia and actin arcs guide the assembly and transport of two populations of microtubules with unique dynamic parameters in neuronal growth cones. J. Cell Biol. *158*, 139–152.

4. Dehmelt, L., and Halpain, S. (2004). Actin and microtubules in neurite initiation: are MAPs the missing link? J. Neurobiol. *58*, 18–33.

5. Drewes, G., Ebneth, A., and Mandelkow, E.M. (1998). MAPs, MARKs and microtubule dynamics. Trends Biochem. Sci. *23*, 307–311.

6. Drechsel, D.N., Hyman, A.A., Cobb, M.H., and Kirschner, M.W. (1992). Modulation of the dynamic instability of tubulin assembly by the microtubule-associated protein tau. Mol. Biol. Cell *3*, 1141–1154.

7. Kowalski, R.J., and Williams, R.C., Jr. (1993). Microtubule-associated protein 2 alters the dynamic properties of microtubule assembly and disassembly. J. Biol. Chem. *268*, 9847–9855.

8. Gamblin, T.C., Nachmanoff, K., Halpain, S., and Williams, R.C., Jr. (1996). Recombinant microtubule-associated protein 2c reduces the dynamic instability of individual microtubules. Biochemistry *35*, 12576–12586.

9. Griffith, L.M., and Pollard, T.D. (1982). The interaction of actin filaments with microtubules and microtubule-associated proteins. J. Biol. Chem. *257*, 9143–9151.

10. Selden, S.C., and Pollard, T.D. (1983). Phosphorylation of micro-tubule-associated proteins regulates their interaction with actin filaments. J. Biol. Chem. *258*, 7064–7071.

11. Kotani, S., Nishida, E., Kumagai, H., and Sakai, H. (1985). Cal-modulin inhibits interaction of actin with MAP2 and Tau, two major microtubule-associated proteins. J. Biol. Chem. *260*, 10779–10783.

12. Sattilaro, R.F. (1986). Interaction of microtubule-associated pro-tein 2 with actin filaments. Biochemistry *25*, 2003–2009.

13. Correas, I., Padilla, R., and Avila, J. (1990). The tubulin-binding sequence of brain microtubule-associated proteins, tau and MAP-2, is also involved in actin binding. Biochem. J. *269*, 61–64.

14. Moraga, D.M., Nunez, P., Garrido, J., and Maccioni, R.B. (1993). A tau fragment containing a repetitive sequence induces bundling of actin filaments. J. Neurochem. *61*, 979–986.

15. Cunningham, C.C., Leclerc, N., Flanagan, L.A., Lu, M., Janmey, P.A., and Kosik, K.S. (1997). Microtubule-associated protein 2c reorganizes both microtubules and microfilaments into distinct cytological structures in an actin-binding protein-280-deficient melanoma cell line. J. Cell Biol. *136*, 845–857.

16. Ackmann, M., Wiech, H., and Mandelkow, E. (2000). Nonsatura-ble binding indicates clustering of tau on the microtubule sur-face in a paired helical filament-like conformation. J. Biol. Chem. *275*, 30335–30343.

17. Kaech, S., Fischer, M., Doll, T., and Matus, A. (1997). Isoform specificity in the relationship of actin to dendritic spines. J. Neurosci. *17*, 9565–9572.

18. Allen, P.G., Shuster, C.B., Kas, J., Chaponnier, C., Janmey, P.A., and Herman, I.M. (1996). Phalloidin binding and rheological dif-ferences among actin isoforms. Biochemistry *35*, 14062–14069.

19. Lewis, S.A., Wang, D.H., and Cowan, N.J. (1988). Microtubule-associated protein MAP2 shares a microtubule binding motif with tau protein. Science *242*, 936–939.

20. Meyer, R.K., and Aebi, U. (1990). Bundling of actin filaments by alpha-actinin depends on its molecular length. J. Cell Biol. *110*, 2013–2024.

21. Dehmelt, L., Smart, F.M., Ozer, R.S., and Halpain, S. (2003). The role of microtubule associated protein 2c in the reorganization of microtubules and lamellipodia during neurite initiation. J. Neurosci. *23*, 9479–9490.

22. Wu, G., Fang, Y., Lu, Z.H., and Ledeen, R.W. (1998). Induction of axon-like and dendrite-like processes in neuroblastoma cells. J. Neurocytol. *27*, 1–14.

23. Makrides, V., Shen, T.E., Bhatia, R., Smith, B.L., Thimm, J., Lal, R., and Feinstein, S.C. (2003). Microtubule-dependent oligomer-ization of tau. Implications for physiological tau function and tauopathies. J. Biol. Chem. *278*, 33298–33304.

24. Voter, W.A., and Erickson, H.P. (1982). Electron microscopy of MAP 2 (microtubule-associated protein 2). J. Ultrastruct. Res. *80*, 374–382.

25. Al-Bassam, J., Ozer, R.S., Safer, D., Halpain, S., and Milligan, R.A. (2002). MAP2 and tau bind longitudinally along the outer ridges of microtubule protofilaments. J. Cell Biol. *157*, 1187–1196.

26. Svitkina, T.M., Verkhovsky, A.B., and Borisy, G.G. (1996). Plectin sidearms mediate interaction of intermediate filaments with mi-crotubules and other components of the cytoskeleton. J. Cell Biol. *135*, 991–1007.

27. Togel, M., Wiche, G., and Propst, F. (1998). Novel features of the light chain of microtubule-associated protein MAP1B: mi-crotubule stabilization, self interaction, actin filament binding, and regulation by the heavy chain. J. Cell Biol. *143*, 695–707.

28. Yang, Y., Bauer, C., Strasser, G., Wollman, R., Julien, J.P., and Fuchs, E. (1999). Integrators of the cytoskeleton that stabilize microtubules. Cell *98*, 229–238.

29. Wille, H., Mandelkow, E.M., and Mandelkow, E. (1992). The juve-nile microtubule-associated protein MAP2c is a rod-like mole-cule that forms antiparallel dimers. J. Biol. Chem. *267*, 10737–10742.

30. DeTure, M.A., Zhang, E.Y., Bubb, M.R., and Purich, D.L. (1996). In vitro polymerization of embryonic MAP-2c and fragments of the MAP-2 microtubule binding region into structures resem-bling paired helical filaments. J. Biol. Chem. *271*, 32702–32706.

31. Caceres, A., and Kosik, K.S. (1990). Inhibition of neurite polarity by tau antisense oligonucleotides in primary cerebellar neurons. Nature *343*, 461–463.

32. Caceres, A., Mautino, J., and Kosik, K.S. (1992). Suppression of MAP2 in cultured cerebellar macroneurons inhibits minor neurite formation. Neuron *9*, 607–618.

33. Gonzalez-Billault, C., Engelke, M., Jimenez-Mateos, E.M., Wan-dosell, F., Caceres, A., and Avila, J. (2002). Participation of struc-tural microtubule-associated proteins (MAPs) in the develop-ment of neuronal polarity. J. Neurosci. Res. *67*, 713–719.

34. Biernat, J., Wu, Y.Z., Timm, T., Zheng-Fischhofer, Q., Mandel-kow, E., Meijer, L., and Mandelkow, E.M. (2002). Protein kinase MARK/PAR-1 is required for neurite outgrowth and establish-ment of neuronal polarity. Mol. Biol. Cell *13*, 4013–4028.

35. Crowther, R.A., and Goedert, M. (2000). Abnormal tau-con-taining filaments in neurodegenerative diseases. J. Struct. Biol. *130*, 271–279.

36. Yao, T.M., Tomoo, K., Ishida, T., Hasegawa, H., Sasaki, M., and Taniguchi, T. (2003). Aggregation analysis of the microtubule binding domain in tau protein by spectroscopic methods. J. Biochem. (Tokyo) *134*, 91–99.

37. Kaech, S., Parmar, H., Roelandse, M., Bornmann, C., and Matus, A. (2001). Cytoskeletal microdifferentiation: a mechanism for organizing morphological plasticity in dendrites. Proc. Natl. Acad. Sci. USA *98*, 7086–7092.

38. Morales, M., and Fifkova, E. (1989). Distribution of MAP2 in dendritic spines and its colocalization with actin. An immuno-gold electron-microscope study. Cell Tissue Res. *256*, 447–456.

39. Ozer, R.S., and Halpain, S. (2000). Phosphorylation-dependent localization of microtubule-associated protein MAP2c to the actin cytoskeleton. Mol. Biol. Cell *11*, 3573–3587.

40. Zhou, F.Q., Waterman-Storer, C.M., and Cohan, C.S. (2002). Focal loss of actin bundles causes microtubule redistribution and growth cone turning. J. Cell Biol. *157*, 839–849.

41. Lim, R.W., and Halpain, S. (2000). Regulated association of mi-crotubule-associated protein 2 (MAP2) with Src and Grb2: evi-dence for MAP2 as a scaffolding protein. J. Biol. Chem. *275*, 20578–20587.